Electronic Supplementary Information

Nanocellulose/polypyrrole aerogel electrodes with higher conductivity via adding vapor grown nano-carbon fiber as conducting networks for supercapacitor application

Yanping Chen,[a,b] Shaoyi Lyu,*[b] Shenjie Han,[b] Zhilin Chen,[b] Wenjun Wang*[a] and Siqun Wang[c,b]

[a] Beijing Engineering Research Center of Cellulose and Its Derivatives, School of Materials Science and Engineering, Beijing Institute of Technology, Beijing 100081, China. Email: wangwenjun@bit.edu.cn

[b] Research Institute of Wood Industry, Chinese Academy of Forestry, Beijing 100091, China. Email: lvsy@caf.ac.cn

[c] Center for Renewable Carbon, University of Tennessee, Knoxville, Tennessee, 37996, USA

1.Supporting Tables

Table S1. Details of the porous properties of CNF/VGCF and CNF/VGCF/PPy aerogels with different VGCF contents

Samples	BET Specific surface area ($m^2\ g^{-1}$)	Average pore diameter (nm)	Total pore volume ($cm^3\ g^{-1}$)
$CNF/VGCF_{0.2}$ aerogel	50.93	10.69	0.1344
$CNF/VGCF_{0.5}$ aerogel	61.51	10.48	0.1547
$CNF/VGCF_{1}$ aerogel	67.18	11.02	0.1728
$CNF/VGCF_{2}$ aerogel	47.81	11.47	0.1338

2.Supporting Figures

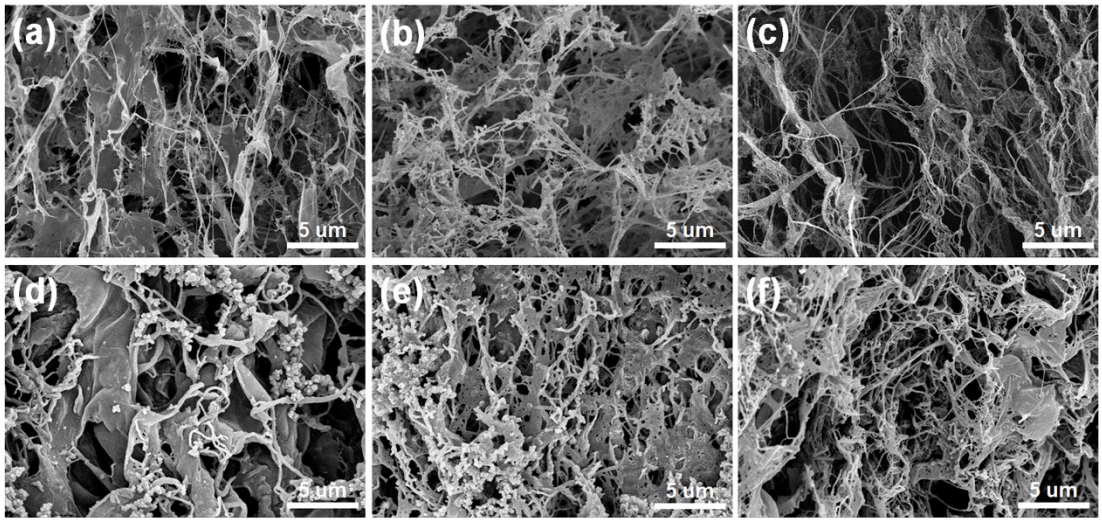

Figure S1. SEM images of (a) $CNF/VGCF_{0.2}$ aerogel, (b) $CNF/VGCF_{0.5}$ aerogel, (c) $CNF/VGCF_2$ aeroge, (d) $CNF/VGCF_{0.2}$/PPy aerogel, (e) $CNF/VGCF_{0.5}$/PPy aerogel, and (f) $CNF/VGCF_2$/PPy aerogel.

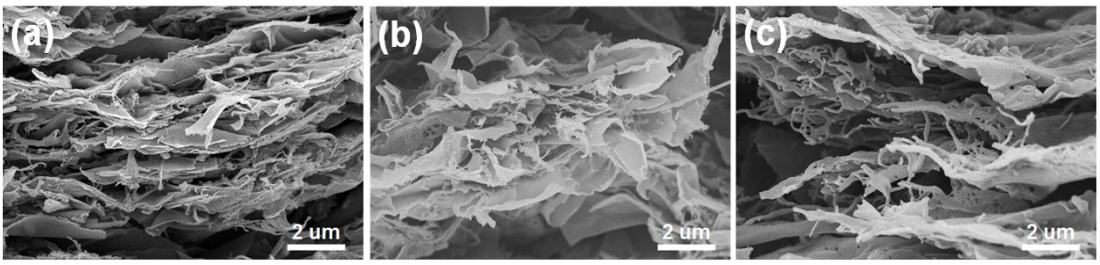

Figure S2. Cross-sectional images of the aerogel films: (a) CNF/VGCF$_{0.2}$/PPy aerogel film, (b) CNF/VGCF$_{0.5}$/PPy aerogel film and (c) CNF/VGCF$_{2}$/PPy aerogel film.

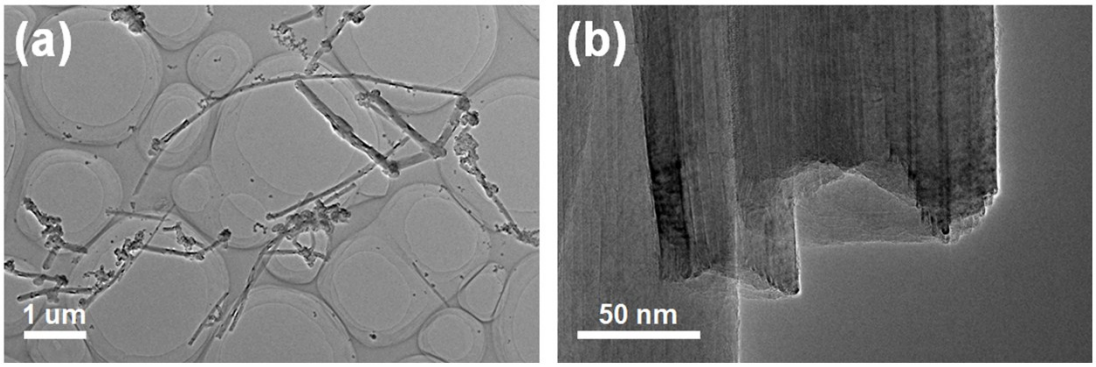

Figure S3. (a) TEM image and (b) a magnified image of VGCF.

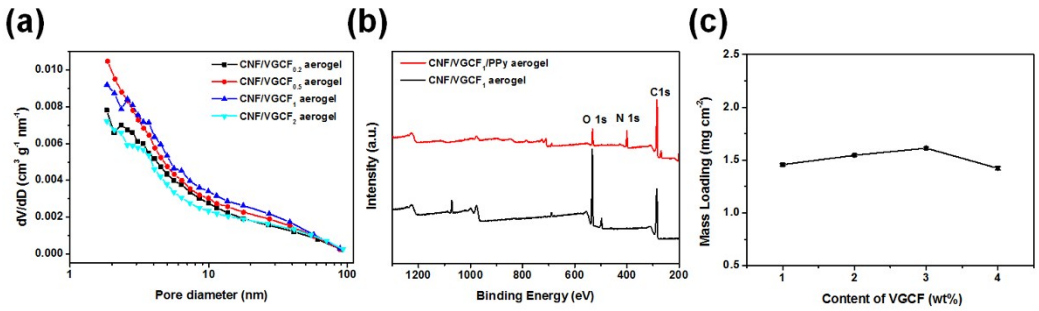

Figure S4. (a) Pore size distributions of CNF/VGCF aerogels with different VGCF contents. (b) XPS wide-region scan spectra of CNF/VGCF$_1$ and CNF/VGCF$_1$/PPy aerogels. (c) PPy mass loading of CNF/VGCF/PPy aerogel with different VGCF contents.

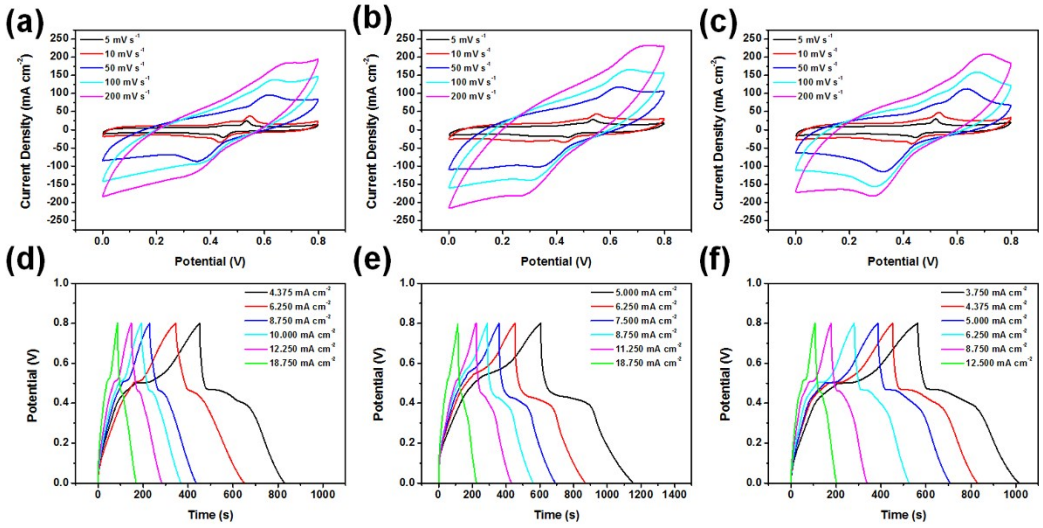

Figure S5. CV curves of (a) CNF/VGCF$_{0.2}$/PPy, (b) CNF/VGCF$_{0.5}$/PPy and (c) CNF/VGCF$_2$/PPy aerogel electrodes at different scan rates. GCD curves of (d) CNF/VGCF$_{0.2}$/PPy, (e) CNF/VGCF$_{0.5}$/PPy and (f) CNF/VGCF$_2$/PPy aerogel electrodes at different current densities. All data were measured in a three-electrode test.

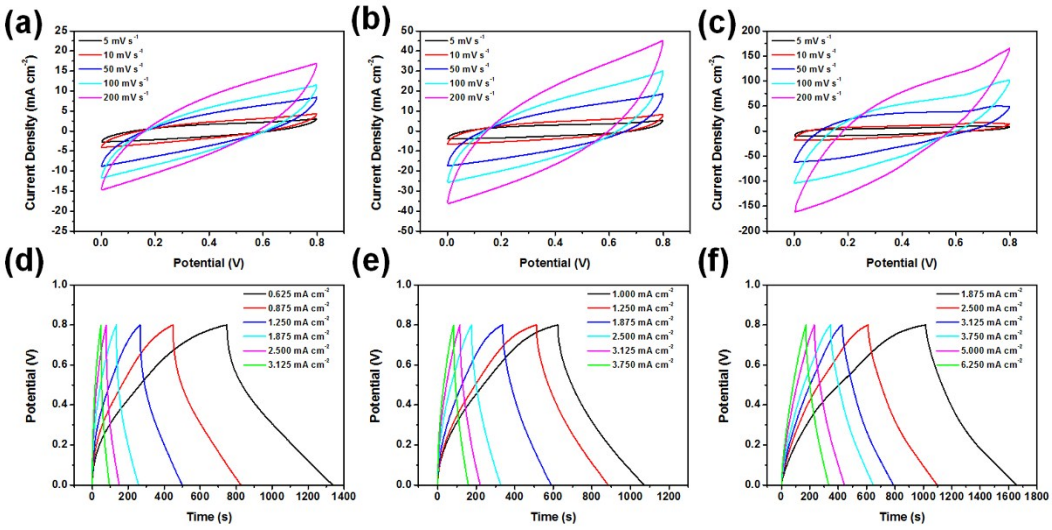

Figure S6. CV curves of (a) CNF/VGCF$_{0.2}$/PPy, (b) CNF/VGCF$_{0.5}$/PPy and (c) CNF/VGCF$_2$/PPy aerogel electrodes at different scan rates. GCD curves of (d) CNF/VGCF$_{0.2}$/PPy, (e) CNF/VGC F$_{0.5}$/PPy and (f) CNF/VGCF$_2$/PPy aerogel electrodes at different current densities. All data were measured in a two-electrode test.

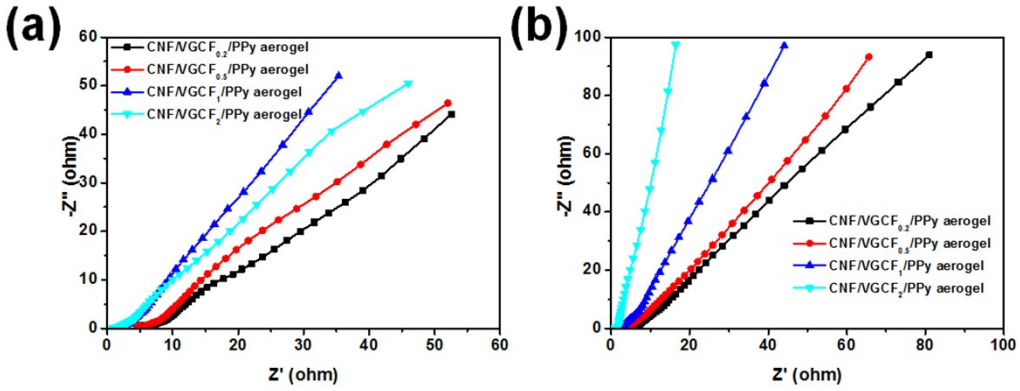

Figure S7. Nyquist impedance plots of CNF/VGCF/PPy aerogel electrodes with different VGCF contents. The data of (a) were measured in a three-electrode test. And the data of (b) were measured in a two-electrode test.

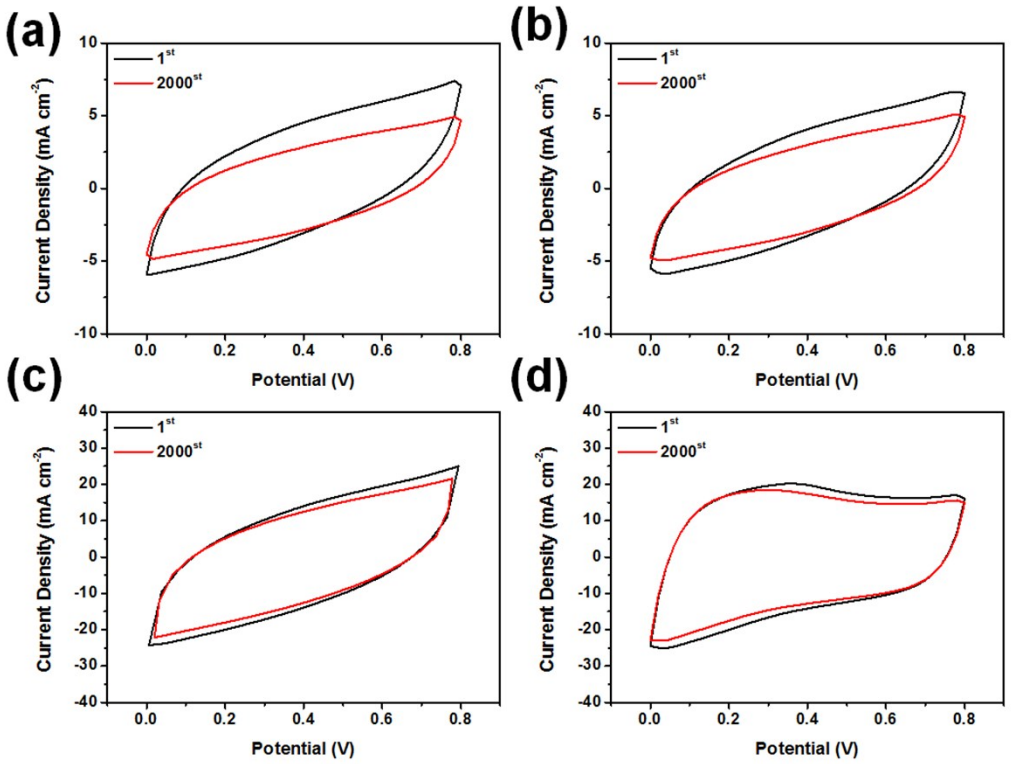

Figure S8. CV curves of (a) CNF/VGCF$_{0.2}$/PPy, (b) CNF/VGCF$_{0.5}$/PPy, (c) CNF/VGCF$_1$/PPy and (d) CNF/VGCF$_2$/PPy aerogel electrodes at 20 mV s^{-1} during cycle-stability testing. All data were measured in a two-electrode test.